Distinct Functions of Nucleotide-Binding/Hydrolysis Sites in the Four AAA Modules of Cytoplasmic Dynein†

Takahide Kon, Masaya Nishiura, Reiko Ohkura, Yoko Y. Toyoshima, and Kazuo Sutoh*

Department of Life Sciences, Graduate School of Arts and Sciences, University of Tokyo, Komaba 3-8-1, Tokyo 153-8902, Japan

Received May 19, 2004; Revised Manuscript Received July 8, 2004

ABSTRACT: Cytoplasmic dynein is a microtubule-based motor protein that is responsible for most intracellular retrograde transports along microtubule filaments. The motor domain of dynein contains six tandemly linked AAA (ATPases associated with diverse cellular activities) modules, with the first four containing predicted nucleotide-binding/hydrolysis sites (P1−P4). To dissect the functions of these multiple nucleotide-binding/hydrolysis sites, we expressed and purified *Dictyostelium* dynein motor domains in which mutations were introduced to block nucleotide binding at each of the four AAA modules, and then examined their detailed biochemical properties. The P1 mutant was trapped in a strong-binding state even in the presence of ATP and lost its motile activity. The P3 mutant also showed a high affinity for microtubules in the presence of ATP and lost most of the microtubule-activated ATPase activity, but retained microtubule sliding activity, although the sliding velocity of the mutant was more than 20-fold slower than that of the wild type. In contrast, mutation in the P2 or P4 site did not affect the apparent binding affinity of the mutant for microtubules in the presence of ATP, but reduced ATPase and microtubule sliding activities. These results indicate that ATP binding and its hydrolysis only at the P1 site are essential for the motor activities of cytoplasmic dynein, and suggest that the other nucleotide-binding/hydrolysis sites regulate the motor activities. Among them, nucleotide binding at the P3 site is not essential but is critical for microtubule-activated ATPase and motile activities of cytoplasmic dynein.

Cytoplasmic dynein is an enormous complex composed of two identical heavy chains (molecular mass of >500 kDa) as well as several intermediate, light intermediate, and light chains and plays an essential role as a molecular motor for chromosomal segregation, mitosis, and most intracellular retrograde transports along microtubules (*1*−*3*). The heavy chain is the central component of the dynein complex, whose ∼1300 N-terminal residues constitute a "stem" domain responsible for dimerization of the heavy chains as well as for binding of associating polypeptide chains (*4*, *5*). The remaining C-terminal ∼380 kDa segment of the heavy chain forms a motor domain that is responsible for most of the motor activities of dynein such as ATP binding and hydrolysis, ATP-sensitive microtubule binding, and active sliding toward the minus ends of microtubules (*6*−*8*). Recent sequence alignments and electron microscopic studies have revealed that the motor domain contains six tandemly linked AAA[1] (ATPases associated with diverse cellular activities) modules that fold into a ring conformation to form a dynein head domain [see Figure 1 (*9*, *10*)]. Unlike the case in other motor proteins, the microtubule-binding region of dynein does not exist within the head domain but is located at the tip of a highly elongated structure called a "stalk" that emerges from the AAA ring (*11*−*14*). Although it has recently been proposed that swinglike motions of the stem and/or the stalk may be responsible for the directed sliding of dynein along microtubules (*15*−*18*), the molecular mechanism underlying the sliding motions of dynein still remains to be elucidated.

Dynein utilizes ATP to slide along the cytoskeletal filament, like other molecular motors such as myosin and kinesin. However, the molecular mechanism of dynein for coupling ATP binding and hydrolysis to generation of the sliding motion is expected to be radically different from those of other molecular motors, since dynein has unique structural and biochemical features (reviewed in refs *15* and *17*). Myosin and kinesin have only a single ATPase site, and ATP hydrolysis there drives the directed sliding of these motors along actin or microtubule filaments. Thus, the intramolecular transmission of information of the ATP hydrolysis cycle at the ATPase site to a molecular apparatus for the sliding motion ("lever arm") is straightforward, even though the molecular details for the process still remain to be established (*19*). In contrast to these molecular motors, sequence analysis of the dynein heavy chains revealed that, among the six AAA modules in the motor domain, the first four contain highly conserved P-loops predicted to bind and/or hydrolyze nucleotides [see Figure 1, P1−P4 (*20*−*23*)]. Consistent with the

† This work was supported by the Grant-in-Aid for Scientific Research (B) from the Ministry of Education, Culture, Sports, Science and Technology of Japan (MEXT) to K.S., by the Core Research for Evolution Science and Technology (CREST) program grant from the Japan Science and Technology Agency (JST) to K.S. and Y.Y.T., and by the Special Coordination Funds for Promoting Science and Technology from MEXT to Y.Y.T.

* To whom correspondence should be addressed. Phone and fax: +81-3-5454-6751. E-mail: sutoh@bio.c.u-tokyo.ac.jp.

[1] Abbreviations: AAA, ATPases associated with diverse cellular activities; CBB, Coomassie Brilliant Blue; GFP, green fluorescent protein; Ni−NTA, nickel nitrilotriacetic acid; PBS, phosphate-buffered saline; PBST, phosphate-buffered saline containing 0.05% Tween 20.

10.1021/bi048985a CCC: $27.50
Published on Web 08/17/2004

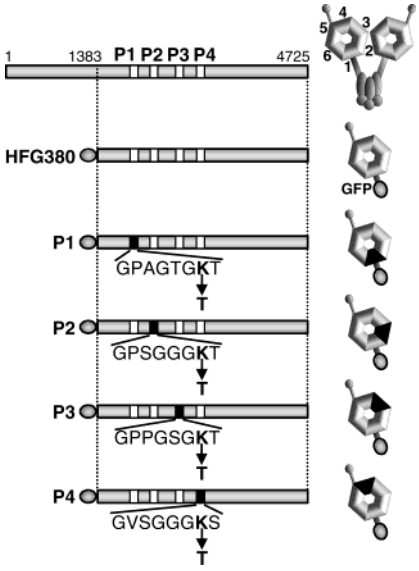

FIGURE 1: Schematic representations of the *Dictyostelium* cytoplasmic dynein heavy chain constructs used in this study. The amino acid residue numbers of the dynein heavy chain are shown on the bar representing its primary sequence. Wild-type and mutagenized P-loops are represented by white and black boxes, respectively. P-Loop sequences are given, and positions of mutations therein are denoted with arrows pointing to the substituted amino acid residue. The N-terminal His_6-FLAG-GFP tag is represented by the gray ovals. For comparison, the full-length 540 kDa dynein heavy chain is shown at the top. Predicted domain structures of the products are shown at the right. Six AAA modules in the motor domain are numbered, and the AAA modules containing mutagenized P-loops are shown in black. It should be noted that each of the first four AAA modules (1−4) contains a P-loop (P1−P4), whereas the other two AAA modules (5 and 6) do not contain this signature sequence.

sequence analysis, it has been shown that an axonemal dynein contains four different ATP-binding sites per heavy chain (*24*). Thus, questions about which ATPase site(s) is primarily responsible for powering the sliding of dynein along microtubule filaments and the functions of these multiple nucleotide-binding/hydrolysis sites arise.

Previous studies on the dynein heavy chains have provided several clues about the functions of these multiple nucleotide-binding/hydrolysis sites in the AAA modules. Kinetic analyses of an axonemal dynein have suggested that there is a single ATPase site per heavy chain (*25*). On the basis of UV-vanadate photocleavage experiments (*26*), it is widely accepted that this ATPase site resides in the first AAA module of the dynein heavy chain. Very recently, it has been shown that *in vivo* functions of the *Drosophila* and yeast cytoplasmic dynein were impaired by P-loop mutations in the first or third AAA module, and the mutations resulted in an ATP-insensitive microtubule binding of the protein (*27*, *28*).

The aim of this study was to elucidate further the functions of the nucleotide-binding/hydrolysis sites in the four AAA modules of the dynein heavy chain by detailed biochemical analyses. To achieve this, we expressed and purified P-loop mutants of the *Dictyostelium* dynein heavy chain and investigated their ATP hydrolysis and microtubule sliding activities as well as their *in vivo* subcellular localization and microtubule binding properties. Our results provide direct biochemical evidence that these four nucleotide-binding/hydrolysis sites have distinct functional roles in the activities responsible for sliding of dynein along microtubule filaments.

MATERIALS AND METHODS

Construction and Transformation. Expression plasmids for wild-type and P-loop mutants of the *Dictyostelium* dynein heavy chain were produced as follows. A DNA fragment encoding the 380 kDa motor domain of the *Dictyostelium* dynein heavy chain (*7*) was excised from pHSG3MB38HG380 (*8*) with *Kpn*I and *Sac*I digestion and ligated into the *Kpn*I−*Sac*I sites of a pHSG3MB38HFG vector to create pHSG-3MB38HFG380. The resulting plasmid contains an HFG380 gene consisting of a His_6 tag, a FLAG tag, and a cDNA of enhanced green fluorescent protein (GFP) followed in-frame by the dynein 380 kDa gene. The HFG380 fragment was then excised from the plasmid with *Mlu*I digestion and subcloned into the *Mlu*I site of an extrachromosomal vector MB38 to create MB38HFG380 for tetracycline-regulated expression in *Dictyostelium* cells (*29*). Site-directed mutations in the four P-loops were created using a QuikChange mutagenesis kit (Stratagene, La Jolla, CA) according to the manufacturer's instruction. To produce the P1 mutant, the codon for K1975 was changed to that for a threonine residue. The P2 (K2277T), P3 (K2675T), P4 (K3017T), and P1/P3 (K1975T/K2675T) mutants were similarly constructed.

Dictyostelium cells used for expression of the dynein genes are derived from the Ax2 strain, in which the expression of a target gene is strongly suppressed if tetracycline is added to the culture medium (*29*). The plasmid carrying the wild-type HFG380 or the P-loop mutant of HFG380 gene was introduced into the *Dictyostelium* cells by electroporation, and transformed cells were selected in HL-5 medium supplemented with 10 μg/mL blasticidin S, 10 μg/mL G418, and 10 μg/mL tetracycline on culture dishes for 1 week.

Fluorescence Microscopy. When the transformed *Dictyostelium* cells were grown semiconfluently in the medium supplemented with the antibiotics described above on culture dishes, the medium was replaced with one without tetracycline to induce the expression of the recombinant dynein. After being incubated for an additional ~24 h, the cells were transferred to glass-bottom dishes and incubated until they adhered to the dishes. The cells were fixed with 4% formaldehyde in 15 mM PIPES-KOH (pH 7.0) and 2 mM $MgCl_2$ for 10 min at room temperature, permeabilized with 70% ethanol for 5 min at −20 °C, and washed with PBS. After being blocked with 3% BSA in PBST for 15 min, the cells were incubated for 1 h with an anti-tubulin antibody (DM1A, Sigma, St. Louis, MO) diluted 1:300 in PBST containing 3% BSA. After being washed with PBS, the cells were incubated for 1 h with a goat anti-mouse IgG coupled to tetramethylrhodamine isothiocyanate (Jackson Laboratories, West Grove, PA) diluted 1:500 in PBST containing 3% BSA. The cells were then washed with PBS and analyzed with a TE300 fluorescence microscope (Nikon, Tokyo, Japan) equipped with a CSU-10 real-time confocal microscope system (Yokogawa, Tokyo, Japan).

Protein Preparation. The transformed cells were grown at 22 °C with shaking until the cell density reached ~5 × 10^6 cells/mL. The medium was then replaced with one without tetracycline to induce the expression of the recombinant dynein. After being cultivated for an additional ~24 h, the cells were harvested by centrifugation. Approximately

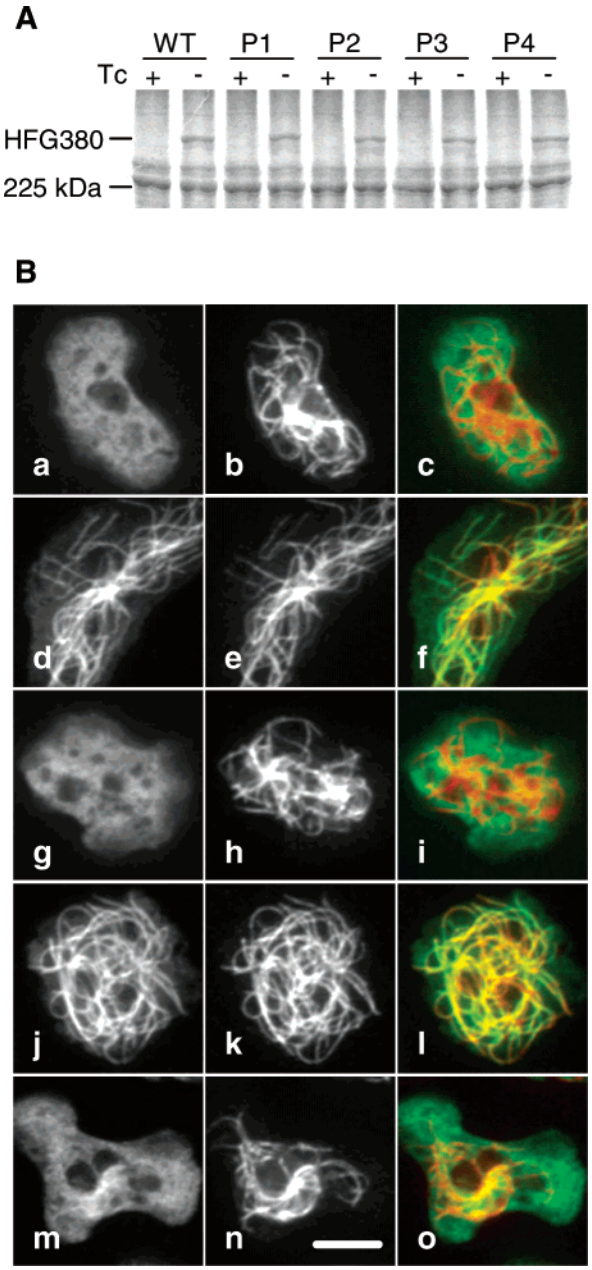

FIGURE 2: Expression and subcellular localization of wild-type HFG380 and its P-loop mutants in *Dictyostelium* cells. (A) Cells transformed with the plasmid encoding wild-type HFG380 (WT) or its P-loop mutant (P1−P4) were cultured in the medium with (+) or without (−) tetracycline (Tc). The whole cell lysates were resolved by SDS−PAGE and stained with CBB. The positions of HFG380 and a 225 kDa molecular mass marker are given at the left. (B) Representative images of the cells expressing wild-type HFG380 (a−c) or the P1 (d−f), P2 (g−i), P3 (j−l), or P4 (m−o) mutant of HFG380. They were fixed and observed under a fluorescence microscope. The GFP fluorescence showed the localization of the HFG380 dyneins (a, d, g, j, and m). Microtubules were visualized with a monoclonal anti-tubulin antibody (b, e, h, k, and n). The corresponding overlaid images are also shown (c, f, i, l, and o). The bar is 5 μm long.

30 g of wet cells harvested from 2 L of culture was used for each preparation. The following purification procedure was carried out at 4 °C or on ice. The cells were lysed with sonication in an equal volume of PMG buffer [100 mM PIPES-KOH, 4 mM $MgCl_2$, 0.1 mM EGTA, 0.9 M glycerol, 1 mM β-mercaptoethanol, 10 μg/mL chymostatin, 10 μg/mL pepstatin, 50 μg/mL leupeptin, 500 μM PMSF, and 0.1 mM ATP (pH 7.0)] supplemented with 10 mM imidazole. The cell lysate was centrifuged at 24000*g* for 20 min, and then the supernatant was centrifuged further at 187000*g* for 60 min. The resulting high-speed supernatant was mixed with 2 mL of nickel nitrilotriacetic acid (Ni−NTA) agarose (Qiagen, Hilden, Germany) in a conical tube on a rotating wheel for 1 h. After the resin had been washed with PMG buffer supplemented with 20 mM imidazole, the adsorbed proteins were eluted four times with PMG buffer supplemented with 250 mM imidazole. The eluted fractions were mixed and loaded onto a PD-10 desalting column (Amersham Biosciences, Piscataway, NJ) to replace the solvent with PMEGS buffer [100 mM PIPES-KOH, 150 mM NaCl, 4 mM $MgCl_2$, 5 mM EGTA, 0.1 mM EDTA, 0.9 M glycerol, 1 mM DTT, 10 μg/mL chymostatin, 10 μg/mL pepstatin, 50 μg/mL leupeptin, 500 μM PMSF, and 0.1 mM ATP (pH 7.0)]. The eluate was mixed with 0.5 mL of FLAG-M2 affinity gel (Sigma) in a conical tube on a rotating wheel for 1 h. After the resin had been washed with PMEG30 buffer [30 mM PIPES-KOH, 4 mM $MgCl_2$, 5 mM EGTA, 0.1 mM EDTA, 0.9 M glycerol, 1 mM DTT, 10 μg/mL chymostatin, 10 μg/mL pepstatin, 50 μg/mL leupeptin, 500 μM PMSF, and 0.1 mM ATP (pH 7.0)], the recombinant dynein was eluted three times with PMEG30 buffer supplemented with 200 μg/mL FLAG peptide (Sigma). The eluates were centrifuged at 356000*g* for 15 min, and the supernatant was used for further study. The purified proteins were stored on ice and used within 3 days. The purity of the recombinant dynein was examined by 5 or 4−20% SDS−PAGE with Coomassie Brilliant Blue (CBB) staining (Simply Blue SafeStain, Invitrogen, Carlsbad, CA) (Figure 3). From 30 g of wet cells, 150−300 μg of the recombinant dynein was obtained.

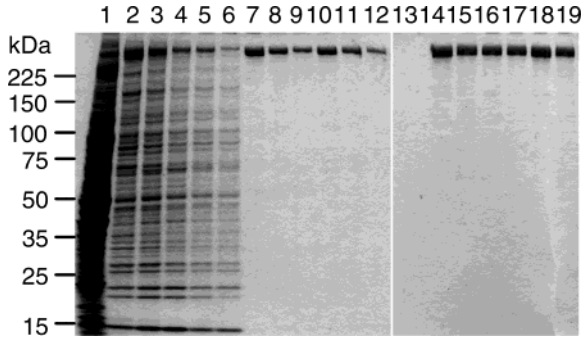

FIGURE 3: Purification of wild-type HFG380 and its P-loop mutants. Samples from each purification step of wild-type HFG380 were resolved by SDS−PAGE and stained with CBB (left): lane 1, high-speed supernatant of the cell lysate; lanes 2−5, four fractions eluted from the Ni−NTA agarose with 250 mM imidazole; lane 6, unbound fraction after incubation with FLAG-M2 affinity gel; lanes 7−9, three fractions eluted from FLAG-M2 affinity gel with 200 μg/mL FLAG peptide; and lanes 10−12, 356000*g* supernatants of the eluted fractions. A CBB-stained SDS−PAGE gel of purified wild-type HFG380 and its P-loop mutants is shown (right): lane 13, a preparation from cells transformed with the empty vector; and lanes 14−19, purified wild-type HFG380 and P1−P4 and P1/P3 mutants, respectively. The numbers at the left denote the positions of the molecular mass markers.

Tubulin was purified from porcine brains as described previously (*30*). Protein concentrations were determined by the Bradford method (Coomassie protein assay reagent, Pierce, Rockford, IL) using BSA as a standard as described

previously (*8*). The microtubule concentration is expressed as the tubulin dimer concentration in all cases in this study.

Vanadate-Mediated Photocleavage. Vanadate-mediated photocleavage was performed essentially as described previously (*26*). Purified dynein (0.25 μM) in PMEG30 buffer was supplemented with 1 mM ATP and 100 μM sodium vanadate and irradiated for 1 h on ice with UV light (365 nm) from a distance of ~1 cm. The photocleavage products were analyzed by SDS−PAGE with CBB staining. Western blotting was carried out by the standard method with an anti-GFP antibody (Clontech, Palo Alto, CA) and a goat anti-rabbit IgG (Amersham Bioscience). An ECL plus system (Amersham Bioscience) was used to detect immunoreactive electrophoretic bands on the blots.

Microtubule Binding Assay. Purified dynein (0.2 μM) in PMEG30 buffer was mixed with paclitaxel-stabilized microtubules (10 μM tubulin dimers) and paclitaxel (40 μM) in the absence or presence of 10 mM ATP. The mixture was incubated for 10 min at 25 °C and centrifuged at 250000*g* for 10 min at 25 °C. The supernatant was saved, and the pellet was resuspended in the same volume of PMEG30 buffer. Both supernatant and pellet fractions were run on a SDS−PAGE gel, and stained with CBB.

Measurements of Basal and Microtubule-Activated ATPase Activities. Basal and microtubule-activated ATPase activities were measured using an EnzChek phosphate assay kit (Molecular Probes, Eugene, OR) in a total volume of 150 μL at 25 °C. Purified dynein (15−25 nM) and various concentrations of paclitaxel-stabilized microtubules (0−40 μM tubulin dimers) were mixed in assay buffer [10 mM PIPES-KOH, 50 mM potassium acetate, 4 mM $MgSO_4$, 1 mM EGTA, 10 μM paclitaxel, and 1 mM DTT (pH 7.0)] supplemented with 1 unit/mL purine nucleoside phosphorylase and 0.2 mM 2-amino-6-mercapto-7-methylpurine riboside, and incubated for 2 min at 25 °C. The reaction was started by addition of ATP and continuously monitored by the absorbance at 360 nm for 5 min. For determination of steady state kinetics as a function of the microtubule concentration expressed as the tubulin dimer concentration, ATP was used at a saturating concentration of 1 mM. For determination of K_m(ATP), a constant concentration of microtubules (10 μM tubulin dimers) and various concentrations of ATP (0−2 mM) were used. The ATPase assay was repeated three times with at least two different dynein preparations. The ATPase rates were calculated from fits to the linear part of the time traces. As controls, the rates of phosphate release from various amounts of microtubules alone without dynein were determined. The values were subtracted from the observed ATPase rates in the presence of the dyneins, although they were less than 7% of the dynein ATPase activities even at the highest microtubule concentrations that were examined. The K_m(MT) and k_{cat} values were obtained from fitting curves based upon the equation $k_{obs} = (k_{cat} - k_{basal})$[tubulin dimer]/[$K_m$(MT) + [tubulin dimer]] + k_{basal}, where k_{obs} and k_{basal} are observed and basal ATPase rates, respectively. The contaminating ATPase activity in our preparations besides the recombinant dynein was estimated by measuring the ATPase rates in a preparation from *Dictyostelium* cells transformed with an empty vector, which was below the level of detection under our assay conditions.

In Vitro Motility Assay. In vitro motility assays were carried out as described previously (*31*) using a flow chamber method with some modifications (*8*). Assays were performed at 25 °C in the ATPase assay buffer without DTT. The assay chamber was sequentially coated with streptavidin (1 mg/mL), protein G-biotin (1 mg/mL), an anti-GFP monoclonal antibody (125 μg/mL, 3E6, Qbiogene, Carlsbad, CA), and BSA (10 mg/mL) by repeating the following three steps: perfusion of the protein into the chamber, incubation for 3 min, and washing of the chamber with 3 chamber volumes of the assay buffer. The purified dynein (~0.4 μM) was then added into the chamber twice at 5 min intervals. After being washed with the assay buffer, the chamber was filled with the assay buffer containing paclitaxel-stabilized microtubules (0.3 μM tubulin dimers) and incubated for 3 min. Finally, the chamber was washed, and then filled with the assay buffer containing 1 mM ATP to initiate microtubule sliding. Microtubules were observed under a BX51 dark-field microscope (Olympus, Tokyo, Japan) equipped with a 40× objective lens. The image was projected onto an ICD-6100 highly sensitive charge-coupled device camera (Ikegami, Tokyo, Japan), contrast-enhanced with an Argus-20 image processor (Hamamatsu Photonics, Hamamatsu, Japan), and recorded with an S-VHS VTR. The recordings were digitized and analyzed. As for the wild type, and P2−P4 mutants, the sliding of microtubules was monitored for 10−180 s so that microtubules moved at least 5 μm. As for P1 mutant, the movements of microtubules were followed for 180 s. At least two independent preparations were analyzed for each mutant. We performed control assays using a preparation from *Dictyostelium* cells transformed with an empty vector, and found that few microtubules attached to the chamber surface, and that their movements were not detected under our assay conditions.

RESULTS

Construction of P-Loop Mutants. Each of the first four AAA modules of the dynein heavy chains contains a highly conserved nucleotide-binding motif (P-loop, or the Walker-A motif), i.e., P1−P4, whose consensus sequence is GXXGXGKT/S. To investigate the functions of the nucleotide-binding/hydrolysis sites in the four AAA modules, the most conserved lysine residue in each of the P-loops was replaced with threonine to generate mutant dyneins (Figure 1). From the many previous mutational studies of P-loops in the Walker-type ATPases, including the AAA^+ superfamily proteins, this type of mutation was predicted to block nucleotide binding at these sites (*32*−*35*).

In this study, we used the 380 kDa motor domain of the *Dictyostelium* dynein heavy chain (*7*) fused with an N-terminal His_6-FLAG-GFP tag as the wild type (HFG380). The K-to-T mutations described above were introduced into HFG380 to generate four mutants (Figure 1). Although another mutation from GK to AS was also introduced in each of the P-loops, the effects of these mutations on the *in vivo* and *in vitro* properties of HFG380 were very similar to those of the K-to-T mutations (data not shown). Therefore, only the K-to-T mutations are described and discussed hereafter.

Expression and Subcellular Localization of Wild-Type HFG380 and Its P-Loop Mutants in Dictyostelium Cells. Before isolating and characterizing the P-loop mutants of HFG380, we first examined their *in vivo* subcellular localization by using the N-terminal GFP as a fluorescence

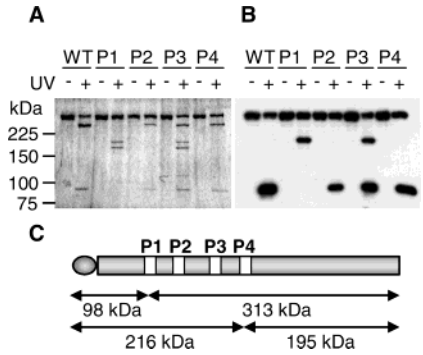

FIGURE 4: Effects of P-loop mutations on the vanadate-mediated photocleavage of HFG380. (A) Purified wild-type HFG380 (WT) or its P-loop mutant (P1−P4) was incubated with 1 mM ATP and 100 μM vanadate for 1 h on ice in the absence (−) or presence (+) of UV irradiation, and analyzed by SDS−PAGE with CBB staining. The numbers at the left are the positions of the molecular mass markers. (B) The appearance of the N-terminal fragments was followed by Western blotting with an anti-GFP antibody. For each wild-type or mutant dynein, we performed the cleavage experiment three times with two independent preparations, and obtained similar results. Representative results are shown. (C) Locations of cleavage sites in HFG380 predicted from the size of the fragments generated by the vanadate-mediated photocleavage reaction.

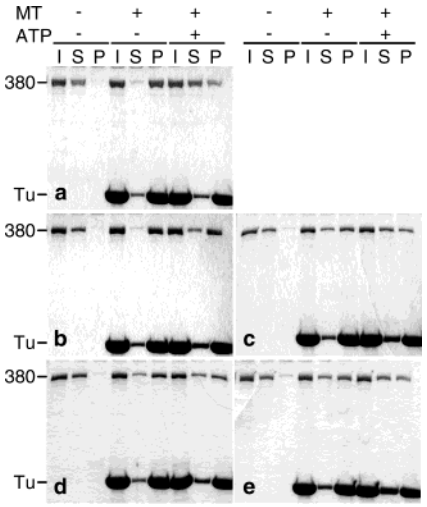

FIGURE 5: Effects of P-loop mutations on microtubule binding of HFG380. Purified wild-type HFG380 (a) or the P1 (b), P2 (c), P3 (d), or P4 (e) mutant of HFG380 was precipitated with (+) or without (−) paclitaxel-stabilized microtubules (MTs) in the absence (−) or presence (+) of ATP and analyzed by SDS−PAGE with CBB staining: I, initial mixture of the dynein and microtubules; S, supernatant after precipitation; and P, pellet after precipitation. The positions of HFG380 (380) and tubulin (Tu) are indicated at the left. For each wild-type or mutant dynein, we performed the coprecipitation experiment three times with two independent preparations, and obtained similar results. Representative results are shown.

marker. Since constitutive expression of some of the mutants was noticed to be unstable in *Dictyostelium* cells, we used the Tet-off system (*29*) to transiently express these GFP-tagged mutants. Twenty-four hours after induction of the expression by removal of tetracycline from the culture medium, all of the recombinant proteins were expressed at similar levels as revealed by SDS−PAGE (Figure 2A). After fixing the cells, we examined the subcellular localization of the mutant dyneins by fluorescence microscopy. Wild-type HFG380 as well as P2 and P4 mutants showed a diffuse distribution throughout the cytoplasm (Figure 2B, panels a−c, g−i, and m−o). As for the P4 mutant, partial colocalization of the mutant with microtubules was also observed. In contrast, P1 and P3 mutants exhibited clear fibrous colocalization with microtubule filaments (Figure 2B, panels d−f and j−l). The results suggest that the P1 or P3 mutation in the dynein heavy chain increases the affinity of the protein for microtubules under *in vivo* conditions.

Purification of Wild-Type HFG380 and Its P-Loop Mutants. For biochemical characterization, we purified wild-type HFG380 and its P-loop mutants. In a previous report, we isolated another type of recombinant 380 kDa motor domain (HG380) by using the sequential steps of His_6 tag affinity and coprecipitation with microtubules (*8*). However, this method was not suitable for purification of the P-loop mutants because some of them were not released effectively from microtubules even in the presence of ATP (Figure 5). Therefore, we used FLAG-M2 affinity for the second purification step in this study. After the first His_6 tag purification step, extra bands besides the main ∼400 kDa band corresponding to the fusion of GFP and the 380 kDa dynein heavy chain on an SDS gel remained (Figure 3, lanes 2−5). These extra bands were eliminated by the second FLAG tag affinity step (Figure 3, lanes 7−9). After ultracentrifugation of the eluted fractions, the supernatant was used for further studies (Figure 3, right panel).

UV Cleavage of Wild-Type HFG380 and Its P-Loop Mutants in the Presence of ATP and Vanadate. It has been shown that the 380 kDa motor domain of the dynein heavy chain, as well as the full-length heavy chains in the dynein complex, is cleaved at the P1 site by UV irradiation in the presence of ATP and vanadate (*6*, *7*, *20*, *21*, *26*). This cleavage reaction is a hallmark of ATP binding and its hydrolysis at the P1 site (*36*). To determine whether the capacity to bind and hydrolyze ATP at the P1 site remained intact in the P-loop mutants, we performed UV-vanadate photocleavage of the purified HFG380 proteins. When wild-type HFG380 was subjected to the reaction, the protein was cleaved into the N-terminal ∼100 kDa and C-terminal ∼300 kDa fragments as revealed by SDS−PAGE and Western blotting (Figure 4A,B, WT). The result showed that the cleavage occurred at the P1 site as expected (Figure 4C).

When the P1 mutant was subjected to UV photocleavage, the N-terminal ∼220 kDa and C-terminal ∼200 kDa fragments were produced in place of the ∼100 and ∼300 kDa fragments (Figure 4A,B, P1). As judged from the size of the fragments that were produced, the new photocleavage site was located possibly close to the P4 site (Figure 4C). Thus, the result suggests that the P1 mutant lost the capacity to bind or hydrolyze ATP at the P1 site but gained the susceptibility to cleavage at the new site. As for the P2 and P4 mutants, the cleavage patterns were the same as that of the wild type (Figure 4A,B, P2 and P4), indicating that the ATP binding and its hydrolysis occurred at the P1 site of these mutants. UV photocleavage of the P3 mutant generated the two sets of fragments (100 kDa + 300 kDa and 220 kDa + 200 kDa) (Figure 4A,B, P3). The fragments in the former set (100 kDa + 300 kDa) correspond to those generated by cleavage at the P1 site of HFG380, and the fragments in the latter one (220 kDa + 200 kDa) are equivalent to those produced by cleavage of the P1 mutant. Therefore, the result indicates that the P3 mutant maintained

the capacity to bind and hydrolyze ATP at the P1 site and suggests that the mutant also gained the susceptibility to cleavage at the same new site as the P1 mutant.

Coprecipitation of Wild-Type HFG380 or Its P-Loop Mutant with Microtubules. To determine if the P-loop mutations affected ATP-sensitive binding of the dynein heavy chain to microtubules, we performed coprecipitation of wild-type or mutant HFG380 with microtubules in the presence or absence of ATP. After precipitation of microtubules, the amounts of bound and unbound HFG380s were determined by SDS−PAGE as shown in Figure 5. As expected, most of the purified wild-type HFG380 precipitated with microtubules in the absence of ATP, whereas approximately two-thirds of the molecules were in the unbound state in the presence of ATP.

As for the P1 mutant, the majority precipitated with microtubules in the presence as well as in the absence of ATP. The result indicates that the P1 mutation resulted in a strong binding of the HFG380 protein to microtubules irrespective of ATP concentrations. This ATP-insensitive strong binding to microtubules is consistent with *in vivo* subcellular localization of the P1 mutant (Figure 2B). The P3 mutant also showed the ATP-insensitive coprecipitation with microtubules such as the case of the P1 mutant, consistent again with its *in vivo* subcellular localization (Figure 2B).

The P2 and P4 mutants exhibited coprecipitation patterns different from those of the other two mutants. Even in the absence of ATP, these mutants bound to microtubules rather weakly as revealed by the presence of unbound mutant proteins. In the presence of ATP, approximately half of the input proteins remained bound to microtubules. Because of the ambiguity in the behavior of the P2 and P4 mutants, it is difficult to determine the effects of these mutations on microtubule binding properties of HFG380, although the results of the coprecipitation assay were reproducible under our assay conditions (see the figure legend).

Basal and Microtubule-Activated ATPase Activities of Wild-Type HFG380 and Its P-Loop Mutants. We measured the basal and microtubule-activated ATPase activities of purified wild-type HFG380 and its P-loop mutants (Figure 6 and Table 1). The basal ATPase activity of HFG380 (5.7 s^{-1}) was activated more than 10-fold on addition of ~4 mg/mL microtubules (40 μM tubulin dimers). The microtubule-activated ATPase activities (the total ATPase activity minus the basal activity) of HFG380 at varying microtubule concentrations expressed as tubulin dimer concentrations were fitted well with a Michaelis−Menten equation that assumed microtubules as pseudosubstrates (Figure 6A). The k_{cat} value, i.e., the maximally activated ATPase activity at an infinite concentration of microtubules, was calculated to be 120 s^{-1}. The K_m(MT) value, i.e., the microtubule concentration at the half-maximal ATPase activity, was 31 μM (Table 1).

As far as the patterns of microtubule-activated ATPase activities are concerned, the P-loop mutants are grouped into two types. The P2 and P4 mutants exhibited microtubule activation patterns similar to that of the wild type (Figure 6C,E). The K_m(MT) values of these mutants as well as that of the wild type were in the range of 10−35 μM (Table 1). However, the basal and microtubule-activated ATPase activities of the mutants were significantly lower than those of the wild type, particularly for the P4 mutant. The basal rates of the P2 and P4 mutants were 2.1 and 0.9 s^{-1}, respectively, whereas that of the wild type was 5.7 s^{-1}. The k_{cat} values of the P2 and P4 mutants were 30 and 5.1 s^{-1}, respectively, whereas that of the wild type was 120 s^{-1}. These results indicate that the P2 or P4 mutation reduced the ATPase rates of HFG380 without affecting its apparent affinity for microtubules in the presence of ATP.

The P1 and P3 mutants exhibited microtubule activation patterns clearly different from that of the wild type (Figure 6B,D). Both retained rather high basal activities (~3 s^{-1}; ~50% of the wild-type rate), but lost most of the microtubule-activated ATPase activities (Table 1). Moreover, the

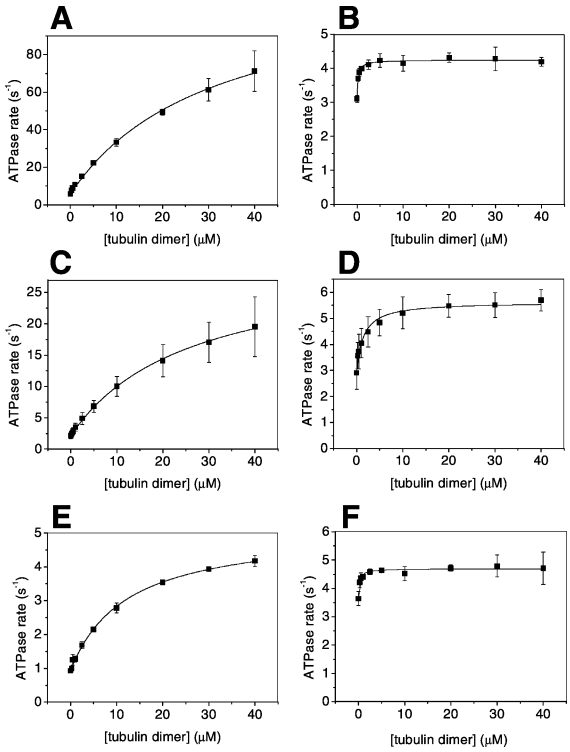

FIGURE 6: Effects of P-loop mutations on the basal and microtubule-activated ATPase activities of HFG380. Steady state ATPase rates of wild-type HFG380 (A) or the P1 (B), P2 (C), P3 (D), P4 (E), or P1/P3 (F) mutant of HFG380 were measured as a function of the microtubule concentration expressed as the tubulin dimer concentration. Each dot is an average value of three independent measurements. Error bars give the standard deviation. Solid lines are the fitting curves based upon the equation $k_{obs} = (k_{cat} - k_{basal})$-[tubulin dimer]/[$K_m$(MT) + [tubulin dimer]] + k_{basal}. According to the analysis, k_{cat} and K_m(MT) values were obtained as shown in Table 1.

Table 1: Summary of ATPase Kinetics of the Wild Type and P-Loop Mutants

	basal ATPase (s^{-1})	microtubule-activated ATPase		
		k_{cat} (s^{-1})	K_m(MT) (μM)	K_m(ATP)[a] (μM)
HFG380	5.7 ± 0.7	120.3 ± 6.0	31.1 ± 3.0	18 ± 2
P1	3.1 ± 0.1	4.3 ± 0.0	0.2 ± 0.0	16 ± 3
P2	2.1 ± 0.4	30.3 ± 1.0	25.8 ± 1.9	70 ± 11
P3	2.9 ± 0.6	5.6 ± 0.1	1.5 ± 0.2	38 ± 6
P4	0.9 ± 0.0	5.1 ± 0.1	12.0 ± 0.9	20 ± 2
P1/P3	3.6 ± 0.3	4.7 ± 0.0	0.2 ± 0.0	nd[b]

[a] K_m(ATP) was calculated from the ATPase rates in the presence of microtubules (10 μM tubulin dimers). [b] Not determined.

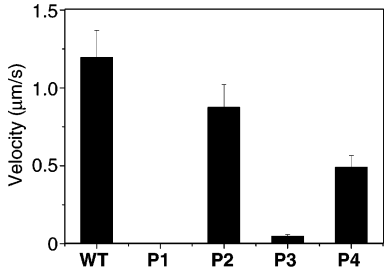

FIGURE 7: Effects of P-loop mutations on the microtubule sliding activity of HFG380. *In vitro* motility assays were performed to examine the microtubule sliding activity of purified wild-type HFG380 (WT) or its P-loop mutants (P1−P4). Measurements were taken with 22−34 microtubules to obtain an average velocity for the preparation. Error bars give the standard deviation.

K_m(MT) values of these mutants (0.2 and 1.5 μM for the P1 and P3 mutants, respectively) were more than 20-fold lower than that of the wild type (31 μM), indicating that apparent affinities of the mutants for microtubules were considerably high even in the presence of ATP. The results are consistent with the observation that the P1 and P3 mutants showed an ATP-insensitive strong binding to microtubules (Figure 5).

A double mutant of P1 and P3 (P1/P3) also exhibited a microtubule activation pattern similar to those of the P1 and P3 single mutants (Figure 6F). It should be noted that not only the microtubule activation patterns but also the values of the ATPase activities of the P1, P3, and P1/P3 mutants were close to one another (Table 1). The effects of the P1 or P3 mutation on the ATPase activities of HFG380 are discussed in the Discussion.

Microtubule Sliding Activities of Wild-Type HFG380 and Its P-Loop Mutants. We examined the motility of microtubule filaments on the purified wild-type HFG380 and its P-loop mutants (Figure 7). Wild-type HFG380 drove sliding of microtubule filaments at an average rate of 1.2 μm/s, whereas the P2 and P4 mutants drove the sliding at rates of 0.9 and 0.5 μm/s, respectively. The P3 mutant also retained the microtubule sliding activity, although the sliding velocity of the mutant (0.05 μm/s) was more than 20-fold slower than that of the wild type. The results indicate that nucleotide binding at the P2, P3, or P4 site is not essential for the sliding of dynein along microtubule filaments. Unlike the cases of these mutants, the sliding of microtubule filaments was not detected on the P1 mutant-coated chamber surface under our assay conditions, indicating that ATP binding and its hydrolysis only at the P1 site are essential for the driving of the sliding of microtubule filaments by dynein.

DISCUSSION

Unlike other motor proteins, dynein contains four nucleotide-binding/hydrolysis sites in its motor domain, and previous reports showed that nucleotide binding and/or hydrolysis at several of the sites was required for *in vivo* dynein functions and for ATP-induced release of dynein from microtubules (*12*, *27*, *28*). However, participation of each of the nucleotide-binding/hydrolysis sites in dynein's motile activities has not been directly evaluated. This report contains the first biochemical demonstration of the functional significance of the multiple nucleotide-binding/hydrolysis sites in dynein's motor activities such as microtubule sliding and ATPase activities by using the purified dynein mutants.

Our results showed that the P1 mutant lost its microtubule sliding activity and was trapped in a strong-binding state even in the presence of ATP. It is generally accepted that P1 is the primary ATPase site of the dynein heavy chain. This was first proposed on the basis of the UV-vanadate cleavage experiments (*26*): the photocleavage of the dynein heavy chain at the P1 site correlated well with loss of its ATPase activity. Recent studies have shown that the P1 mutation in the rat, *Drosophila*, or yeast cytoplasmic dynein heavy chain caused a rigor-like microtubule binding of the mutant dynein and loss of its *in vivo* functions (*12*, *27*, *28*). Our biochemical data for the P1 mutant are consistent with these previous reports and directly demonstrate that ATP binding and its hydrolysis only at the P1 site are essential for the motile activity of cytoplasmic dynein.

The P1 mutation, however, did not result in a complete loss of ATPase activity, and the mutant still retained a high level of basal ATPase activity. It is unlikely that this mutation was leaky, and did not completely inhibit the ATP hydrolysis at the P1 site, considering our observation that the UV-vanadate cleavage at the site was completely blocked in the P1 mutant. Therefore, the results suggest a possibility that, besides P1, there is another ATPase site(s) in some of the AAA modules of the dynein heavy chain. Since the P1/P3 double mutant retained basal and microtubule-activated ATPase activities similar to those of the P1 mutant, it seems unlikely that the third AAA module is mainly responsible for the remaining ATPase activity of the P1 mutant. Therefore, the second and/or fourth AAA modules of the dynein heavy chain may have this ATPase activity. In this context, it should be noted that the UV-vanadate treatment generated a pair of products cleaved possibly close to the P4 site when the P1 or P3 mutation was introduced.

Like the P1 mutant, the P3 mutants also exhibited high affinity for microtubules even in the presence of ATP as revealed by its *in vivo* subcellular localization and microtubule binding properties of the purified mutant protein, which is consistent with previous reports on P3 mutants of *Drosophila* and yeast cytoplasmic dyneins (*27*, *28*). Our ATPase data for the P3 mutant showed that the K_m(MT) value of the mutant was more than 20-fold lower than that of the wild type, reflecting the high affinity of the mutant protein for microtubules in the presence of ATP, and that the mutant lost most of microtubule-activated ATPase activity. These results indicate that the function of the P3 site is critical for ATP-induced release of dynein from microtubules and for microtubule-induced activation of ATPase activity. However, the P1 site of the P3 mutant was cleaved by the UV-vanadate treatment, suggesting that ATP hydrolysis at the primary ATPase site was not blocked by the P3 mutation. Furthermore, the P3 mutant retained microtubule sliding activity, although the sliding rate of the mutant was more than 20-fold slower than that of the wild type. Taken together, these results suggest that the P3 mutation does not completely block the ATPase activity at the P1 site but slows the ATPase cycle at strong-binding step(s) in such a way that the mutant molecules accumulate at strong-binding state(s) during the steady state ATP hydrolysis. Therefore, it is likely that the nucleotide binding or hydrolysis at the P3 site should increase the microtubule-

activated ATPase activity at the P1 site and, as a consequence, markedly promote the microtubule sliding activity. Similar highly cooperative behaviors of multiple ATPase sites have been observed in several hetero-oligomeric AAA complexes (reviewed in ref *16*).

Our biochemical analyses of the P4 mutant predict that this site has a regulatory role in the motile activity of cytoplasmic dynein. The function of the P4 site is not required for the sliding of dynein along microtubules as revealed by the *in vitro* motility assay: the P4 mutant exhibited microtubule sliding activity at ~50% of the wild-type rate. However, the P4 mutant showed only a low level of the microtubule-activated ATPase activity; the k_{cat} value of the mutant was 5.1 s^{-1}, whereas that of the wild type was much higher (120 s^{-1}). These results suggest that nucleotide binding at the fourth AAA module may ensure maximum stimulation of microtubule-activated ATPase activity through an effective coupling between the microtubule-binding site located next to the fourth AAA module and the primary ATPase site in the first AAA module. Since the ratio of the k_{cat} value to the sliding velocity is a function of the duty ratio of the ATPase cycle and the step size (*37*), the modulation of the ATPase cycle at the P1 site induced by the nucleotide binding at the P4 site might be related to the "ATP-regulated gear" that senses force on dynein and modulates its step size on microtubule filaments (*38*).

Since the P2 mutation generated the mildest phenotypic changes in HFG380, it is very likely that the function of the nucleotide-binding/hydrolysis site in the second AAA module is dispensable for the motor activities of cytoplasmic dynein.

In summary, on the basis of biochemical analyses of P-loop mutants, we have provided direct evidence that multiple nucleotide-binding/hydrolysis sites in the four AAA modules of the dynein heavy chain have distinct functions in the motor activities of cytoplasmic dynein. The first AAA module has the primary ATPase site, where ATP hydrolysis is markedly stimulated by microtubules and powers sliding of dynein along microtubule filaments, as previously claimed (*12*, *27*, *28*, *36*). The nucleotide-binding/hydrolysis site in the third AAA module is not essential but is critical for generation of sliding motions, possibly through tight modulation of the ATPase cycle at the primary ATPase site. The second and/or the fourth AAA module(s) may have ATPase site(s), whose activities are not markedly stimulated by microtubules and are not required for the motor activities. Among them, the nucleotide-binding/hydrolysis site in the fourth AAA module seems to play a regulatory role by modulating the efficiency of coupling between the microtubule-binding site and the primary ATPase site.

ACKNOWLEDGMENT

We thank Dr. Peter J. van Haastert (University of Groningen, Groningen, The Netherlands) for providing us with the tetracycline-regulated expression system.

REFERENCES

1. Holzbaur, E. L., and Vallee, R. B. (1994) DYNEINS: molecular structure and cellular function, *Annu. Rev. Cell Biol. 10*, 339−372.
2. Vallee, R. B., and Sheetz, M. P. (1996) Targeting of motor proteins, *Science 271*, 1539−1544.
3. Vale, R. D. (2003) The molecular motor toolbox for intracellular transport, *Cell 112*, 467−480.
4. Habura, A., Tikhonenko, I., Chisholm, R. L., and Koonce, M. P. (1999) Interaction mapping of a dynein heavy chain. Identification of dimerization and intermediate-chain binding domains, *J. Biol. Chem. 274*, 15447−15453.
5. Tynan, S. H., Gee, M. A., and Vallee, R. B. (2000) Distinct but overlapping sites within the cytoplasmic dynein heavy chain for dimerization and for intermediate chain and light intermediate chain binding, *J. Biol. Chem. 275*, 32769−32774.
6. Paschal, B. M., Shpetner, H. S., and Vallee, R. B. (1987) MAP 1C is a microtubule-activated ATPase which translocates microtubules in vitro and has dynein-like properties, *J. Cell Biol. 105*, 1273−1282.
7. Koonce, M. P., and Samso, M. (1996) Overexpression of cytoplasmic dynein's globular head causes a collapse of the interphase microtubule network in *Dictyostelium*, *Mol. Biol. Cell 7*, 935−948.
8. Nishiura, M., Kon, T., Shiroguchi, K., Ohkura, R., Shima, T., Toyoshima, Y., and Sutoh, K. (2004) A single-headed recombinant fragment of *Dictyostelium* cytoplasmic dynein can drive the robust sliding of microtubules, *J. Biol. Chem. 279*, 22799−22902.
9. Samso, M., Radermacher, M., Frank, J., and Koonce, M. P. (1998) Structural characterization of a dynein motor domain, *J. Mol. Biol. 276*, 927−937.
10. Neuwald, A. F., Aravind, L., Spouge, J. L., and Koonin, E. V. (1999) AAA^+: A class of chaperone-like ATPases associated with the assembly, operation, and disassembly of protein complexes, *Genome Res. 9*, 27−43.
11. Goodenough, U., and Heuser, J. (1984) Structural comparison of purified dynein proteins with in situ dynein arms, *J. Mol. Biol. 180*, 1083−1118.
12. Gee, M. A., Heuser, J. E., and Vallee, R. B. (1997) An extended microtubule-binding structure within the dynein motor domain, *Nature 390*, 636−639.
13. Koonce, M. P. (1997) Identification of a microtubule-binding domain in a cytoplasmic dynein heavy chain, *J. Biol. Chem. 272*, 19714−19718.
14. Koonce, M. P., and Tikhonenko, I. (2000) Functional elements within the dynein microtubule-binding domain, *Mol. Biol. Cell 11*, 523−529.
15. King, S. M. (2000) AAA domains and organization of the dynein motor unit, *J. Cell Sci. 113*, 2521−2526.
16. Vale, R. D. (2000) AAA proteins. Lords of the ring, *J. Cell Biol. 150*, F13−F19.
17. Asai, D. J., and Koonce, M. P. (2001) The dynein heavy chain: structure, mechanics and evolution, *Trends Cell Biol. 11*, 196−202.
18. Burgess, S. A., Walker, M. L., Sakakibara, H., Knight, P. J., and Oiwa, K. (2003) Dynein structure and power stroke, *Nature 421*, 715−718.
19. Vale, R. D., and Milligan, R. A. (2000) The way things move: looking under the hood of molecular motor proteins, *Science 288*, 88−95.
20. Gibbons, I. R., Gibbons, B. H., Mocz, G., and Asai, D. J. (1991) Multiple nucleotide-binding sites in the sequence of dynein β heavy chain, *Nature 352*, 640−643.
21. Ogawa, K. (1991) Four ATP-binding sites in the midregion of the β heavy chain of dynein, *Nature 352*, 643−645.
22. Koonce, M. P., Grissom, P. M., and McIntosh, J. R. (1992) Dynein from *Dictyostelium*: primary structure comparisons between a cytoplasmic motor enzyme and flagellar dynein, *J. Cell Biol. 119*, 1597−1604.
23. Mikami, A., Paschal, B. M., Mazumdar, M., and Vallee, R. B. (1993) Molecular cloning of the retrograde transport motor cytoplasmic dynein (MAP 1C), *Neuron 10*, 787−796.
24. Mocz, G., and Gibbons, I. R. (1996) Phase partition analysis of nucleotide binding to axonemal dynein, *Biochemistry 35*, 9204−9211.
25. Shimizu, T., and Johnson, K. A. (1983) Kinetic evidence for multiple dynein ATPase sites, *J. Biol. Chem. 258*, 13841−13846.
26. Gibbons, I. R., Lee-Eiford, A., Mocz, G., Phillipson, C. A., Tang, W. J., and Gibbons, B. H. (1987) Photosensitized cleavage of dynein heavy chains. Cleavage at the "V1 site" by irradiation at 365 nm in the presence of ATP and vanadate, *J. Biol. Chem. 262*, 2780−2786.

27. Silvanovich, A., Li, M. G., Serr, M., Mische, S., and Hays, T. S. (2003) The third P-loop domain in cytoplasmic dynein heavy chain is essential for dynein motor function and ATP-sensitive microtubule binding, *Mol. Biol. Cell 14*, 1355−1365.
28. Reck-Peterson, S. L., and Vale, R. D. (2004) Molecular dissection of the roles of nucleotide binding and hydrolysis in dynein's AAA domains in *Saccharomyces cerevisiae*, *Proc. Natl. Acad. Sci. U.S.A. 101*, 1491−1495.
29. Blaauw, M., Linskens, M. H., and van Haastert, P. J. (2000) Efficient control of gene expression by a tetracycline-dependent transactivator in single *Dictyostelium discoideum* cells, *Gene 252*, 71−82.
30. Sloboda, R. D., and Rosenbaum, J. L. (1982) Purification and assay of microtubule-associated proteins (MAPs), *Methods Enzymol. 85*, 409−416.
31. Vale, R. D., and Toyoshima, Y. Y. (1988) Rotation and translocation of microtubules in vitro induced by dyneins from *Tetrahymena* cilia, *Cell 52*, 459−469.
32. Schirmer, E. C., Queitsch, C., Kowal, A. S., Parsell, D. A., and Lindquist, S. (1998) The ATPase activity of Hsp104, effects of environmental conditions and mutations, *J. Biol. Chem. 273*, 15546−15552.
33. Krzewska, J., Konopa, G., and Liberek, K. (2001) Importance of two ATP-binding sites for oligomerization, ATPase activity and chaperone function of mitochondrial Hsp78 protein, *J. Mol. Biol. 314*, 901−910.
34. Ogura, T., and Wilkinson, A. J. (2001) AAA^+ superfamily ATPases: common structure−diverse function, *Genes Cells 6*, 575−597.
35. Wang, Q., Song, C., Yang, X., and Li, C. C. (2003) D1 ring is stable and nucleotide-independent, whereas D2 ring undergoes major conformational changes during the ATPase cycle of p97-VCP, *J. Biol. Chem. 278*, 32784−32793.
36. Gibbons, I. R. (1995) Dynein family of motor proteins: present status and future questions, *Cell Motil. Cytoskeleton 32*, 136−144.
37. Howard, J. (2001) Speeds of Motors, in *Mechanics of Motor Proteins and the Cytoskeleton*, pp 213−227, Sinauer Associates, Sunderland, MA.
38. Mallik, R., Carter, B. C., Lex, S. A., King, S. J., and Gross, S. P. (2004) Cytoplasmic dynein functions as a gear in response to load, *Nature 427*, 649−652.

BI048985A